SUPPLEMENTARY INFORMATION

Competing mechanisms and scaling laws for carbon nanotube scission by ultrasonication

Guido Pagani[1], Micah J. Green[2], Philippe Poulin[3], Matteo Pasquali[1,*]

[1]Department of Chemical and Biomolecular Engineering, Department of Chemistry, The Smalley Institute for Nanoscale Science & Technology, Rice University, 6100 Main, Houston, TX 77005

[2]Department of Chemical Engineering, Texas Tech University, 6th and Canton, MS3121, Lubbock, TX 79409

[3]Universite de Bordeaux, CNRS, Centre de Recherche Paul Pascal, Avenue Schweitzer, 33600 Pessac, France

*corresponding author, email: mp@rice.edu

List of Variables

k	*scission rate*
k_B	*Boltzmann constant*
T	*Temperature*
L	*CNT length*
L_0	*length of initial (monodisperse) CNT population*
n	*number of CNTs with a given length L*
n_0	*initial (monodisperse) number of CNTs with given length* L_0
a	*constant in dependence on scission rate k on length L*
m	*slope of log(L) vs. log(t),* $m = (-1/q)$
v	*velocity of fluid*
r	*position in space relative to bubble center*
V	*velocity of bubble wall*
v_n	*normal velocity of differential element of a CNT*
R	*radius of bubble wall*
R_i	*initial position of bubble wall*
R_{max}	*maximum position of bubble wall*
R_{crit}	*critical position of bubble wall where adiabatic phase of cycle begins*

F	*force*
F_{tens}	*tensile force on a CNT*
F_c	*critical force for breaking a CNT*
F_j	*force on a BD bead j*
E	*elastic modulus of CNT*
N	*number of beads in Brownian Dynamics simulation*
I_M	*moment of inertia of a CNT*
$y(\xi_c)$	*percentage of CNTs that experience a minimum radius of curvature under* ξ_c
D	*diameter of CNT*
D_t	*translational diffusivity of a CNT of length L*
D_{rot}	*rotational diffusivity of a CNT*
w	*width of CNT wall*
s	*distance along the length of a CNT*
q	*exponent for* $k \sim L^q$
P_A	*acoustic pressure*
P_{A0}	*amplitude of acoustic pressure*
P_{bulk}	*pressure in the bulk fluid*
P_{bubble}	*pressure inside the bubble*
P_v	*vapor pressure of the liquid*
P_{gas}	*partial pressure of the gas inside the bubble*
$P_{gas,0}$	*partial pressure of the gas inside the bubble at time t=0*
t	*time*
t^*	*time / bubble lifetime*
L	*CNT length*
L_p	*CNT persistence length*
d	*distance from CNT center of mass to bubble center*
d_{max}	*maximum d experienced by a CNT*
d_i	*initial d*
$d_{i,c}$	*critical* d_i *(associated with critical maximum strain rate)*
σ	*stress in a CNT*
σ_{break}	*tensile strength of CNT*
$\dot{\varepsilon}$	*strain rate in fluid*
$\dot{\varepsilon}_c$	*critical strain rate necessary to stretch or buckle a CNT*
$\dot{\varepsilon}_{max}$	*maximum strain rate experienced by CNT center of mass during cycle*
α	*parameter describing relationship between onset of buckling and onset of compressive breaking*
β	*slope for log(maximum strain rate) vs. log(*d_i*)*
γ	*surface tension*

ρ	*density of the liquid*
ξ_c	*minimum radius of curvature experienced by a CNT*
$\xi_{c,avg}$	*minimum radius of curvature experienced by a CNT, averaged over all trials*
$\xi_{c,crit}$	*critical breaking value of the minimum radius of curvature experienced by a CNT*
κ	*adiabatic index*
μ	*fluid viscosity*
ω	*sonication frequency*

Supplementary Movie

Mov. S1:

Movie showing an example CNT simulation for P_{A0} = 1500 kPa, d_i = 60 μm, L= 3000 nm, L_p = 50 μm, N = 121. The right graph shows the single-cycle bubble diameter as a function of dimensionless time. On the left, the CNT orientation is shown (the bubble center lies in the $-x$ direction). The CNT begins the collapse in a tangential orientation and remains in that orientation until it buckles. The small radius of curvature in at the end of the bubble collaps suggests that the CNT breaks.

Supplementary Figures

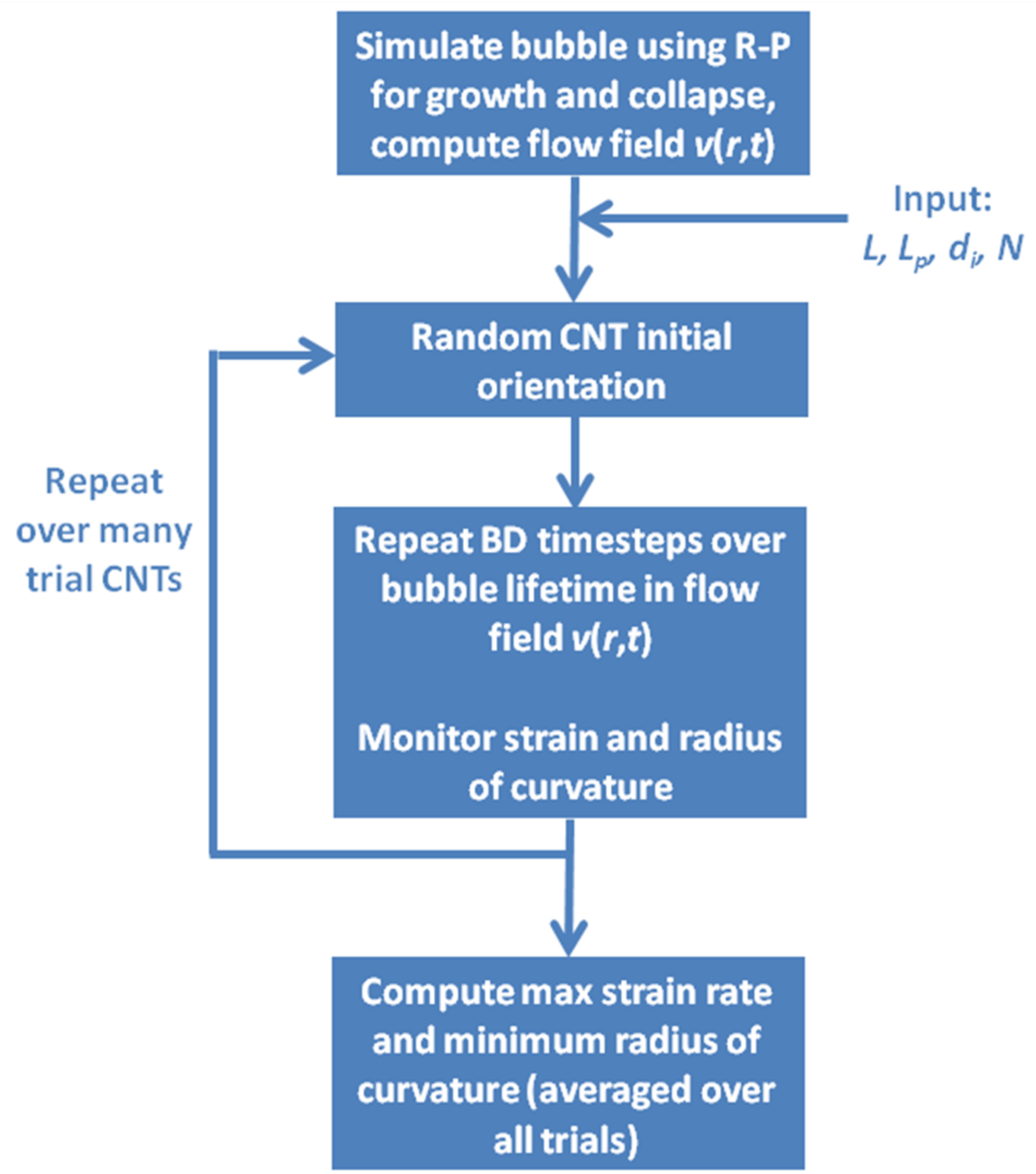

Fig. S1:

Numerical algorithm used to compute the dynamics of CNTs near a cavitating bubble during sonication. The dynamics of the bubble are computed first, and the corresponding flow field drives the Brownian Dynamics simulation of many CNTs for a given parameter set (L, L_p, d_i, N). Full simulation details are given in Refs. [1, 2].

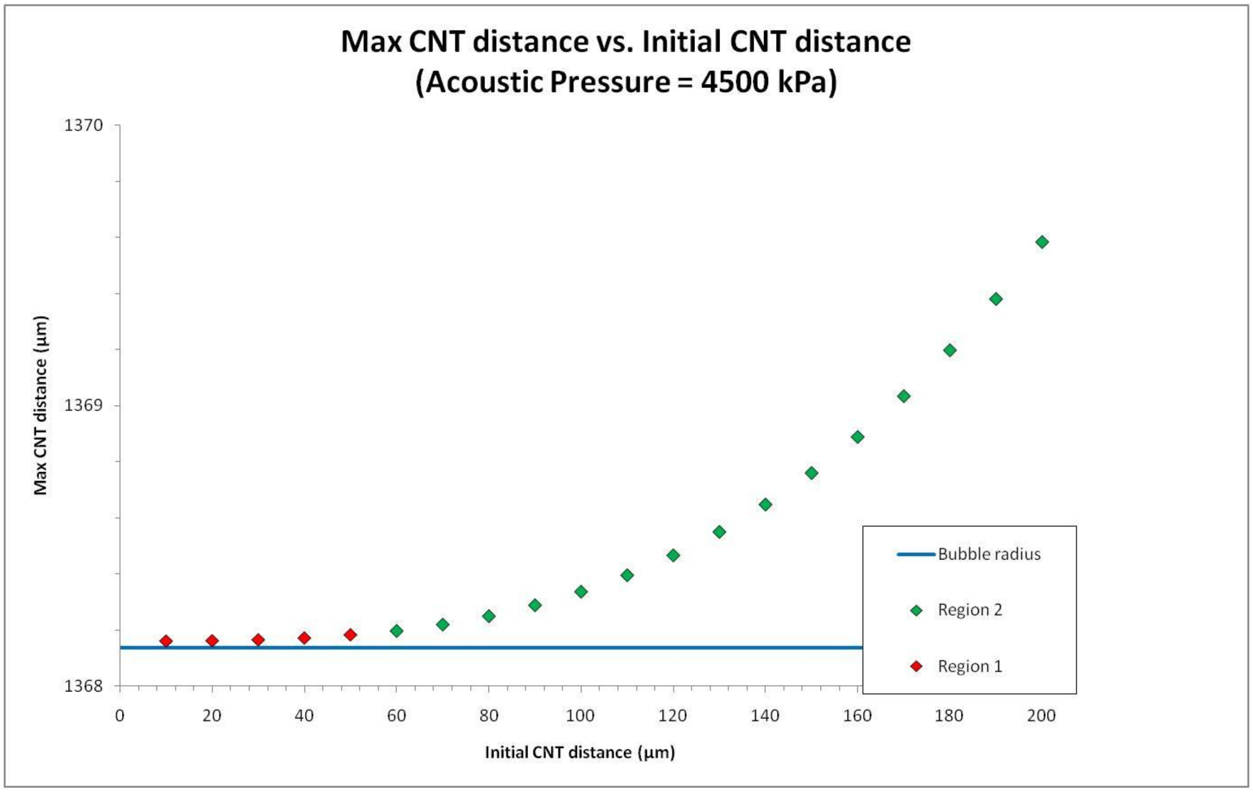

Fig. S2:

The maximum distance of the CNT from the bubble center (at the end of the bubble expansion) plotted against the CNT initial distance from the bubble center. If the initial distance is too small, the CNT is entrained by the advancing bubble wall (Region 1). The initial orientation and random forces are immaterial during bubble growth. Here, P_{A0} = 4500 kPa, L = 1.5 μm, L_p = 20 μm, and N = 33. Similar results are seen for other bubble parameter sets.

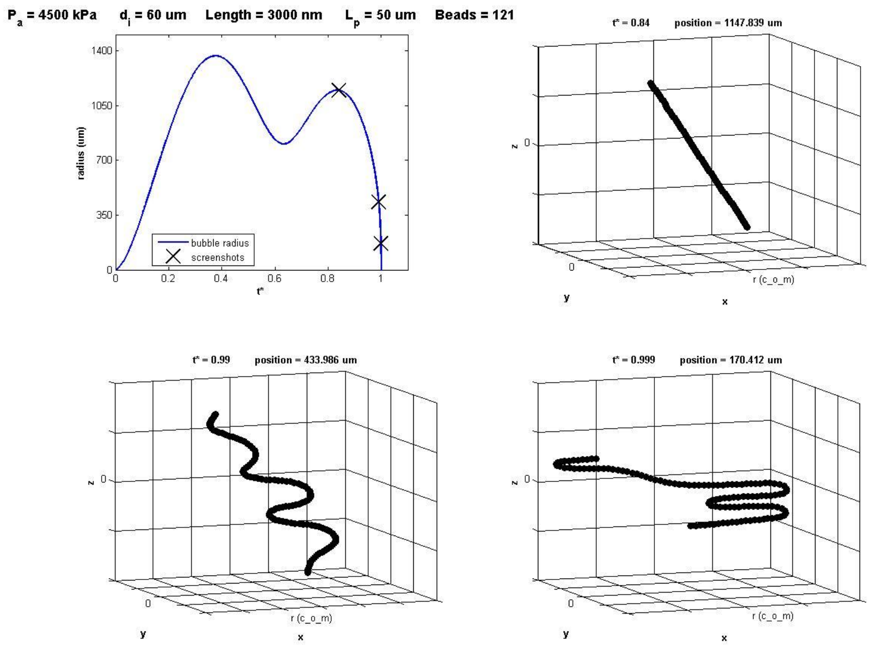

Fig. S3:

A simulation is shown for P_{A0} = 4500 kPa, d_i = 60 μm, L = 3 μm, L_p = 50 μm, N = 121. The upper left graph shows the double-cycle bubble diameter as a function of dimensionless time. Simulation snapshots are shown for the three times marked on the graph. In each snapshot, the bubble center lies in the -*x* direction. The CNT begins in a tangential orientation and remains in that orientation until it undergoes disruptive buckling.

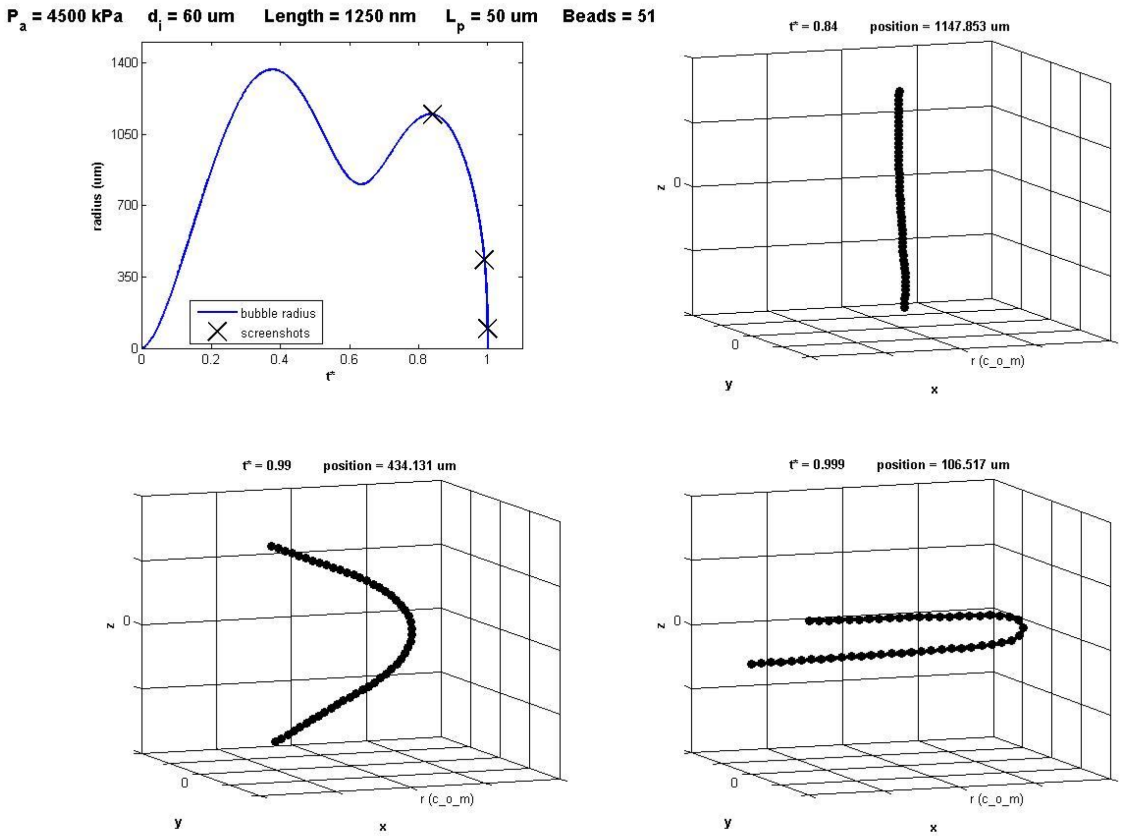

Fig. S4:

A simulation is shown for P_{A0} = 4500 kPa, d_i = 60 μm, L=1250 nm, L_p = 50 μm, N = 51. The upper left graph shows the double-cycle bubble diameter as a function of dimensionless time. Simulation snapshots are shown for the three times marked on the graph. In each snapshot, the bubble center lies in the -x direction. The CNT begins in a tangential orientation and remains in that orientation until it buckles in a specific spot. The small radius of curvature in the final snapshot suggests that the CNT snaps.

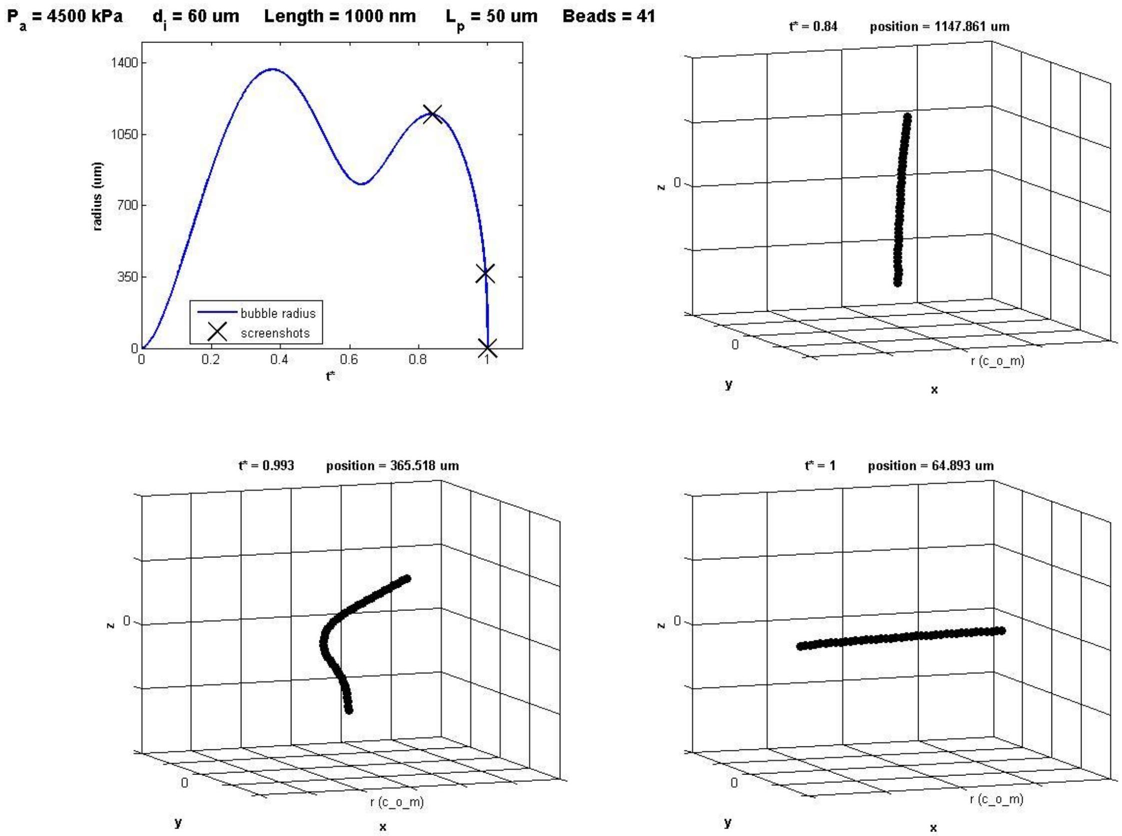

Fig. S5:

A simulation is shown for P_{A0} = 4500 kPa, d_i = 60 μm, L= 1 μm, L_p = 50 μm, N = 41. The upper left graph shows the double-cycle bubble diameter as a function of dimensionless time. Simulation snapshots are shown for the three times marked on the graph. In each snapshot, the bubble center lies in the -x direction. The CNT begins in a tangential orientation and rotates toward a radial orientation while developing only a small degree of curvature. The only way for the radially oriented CNT to break is via stretching.

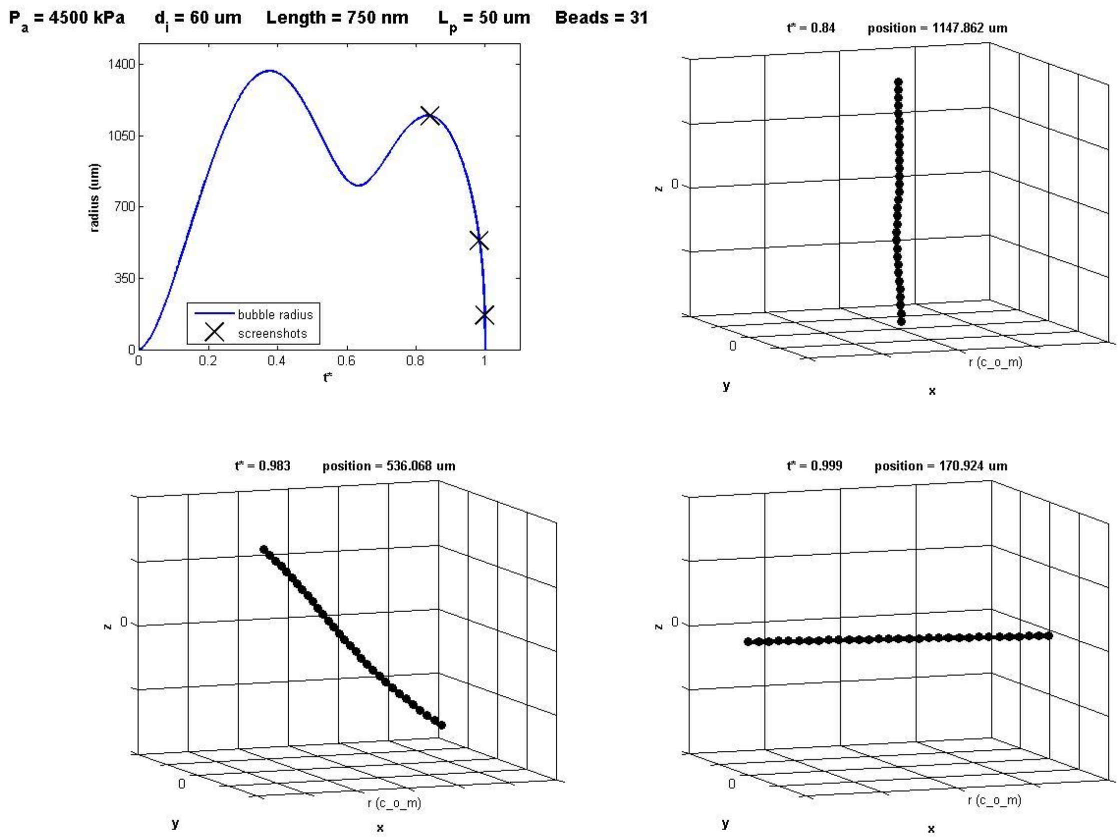

Fig. S6:

A simulation is shown for P_A = 4500 kPa, d_i = 60 µm, L=750 nm, L_p = 50 µm, N = 31. The upper left graph shows the double-cycle bubble diameter as a function of dimensionless time. Simulation snapshots are shown for the three times marked on the graph. In each snapshot, the bubble center lies in the -*x* direction. The CNT begins in a tangential orientation and rigidly rotates toward a radial orientation. The only way for the radially oriented CNT to break is via stretching.

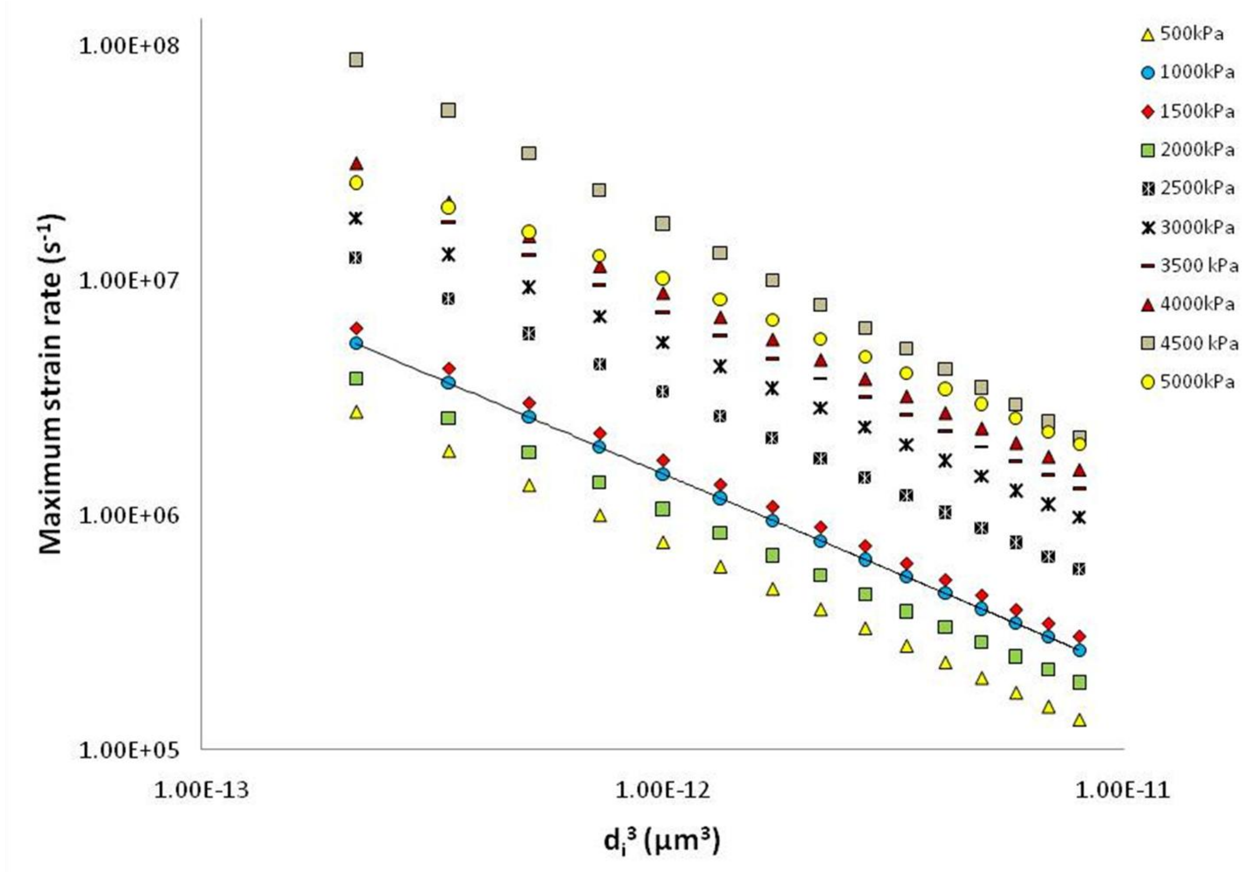

Fig. S7:

The maximum strain rate $\dot{\varepsilon}_{max}$ experienced by a CNT is shown as a function of d_i^3 for several values of P_{A0}. (L = 1.5 µm, L_p = 20 µm, N = 33). This log-log relationship is independent of initial orientation. Note that the maximum strain rate is not monotonic with acoustic pressure P_{A0} because of the transition from a single cycle bubble to a double cycle bubble.

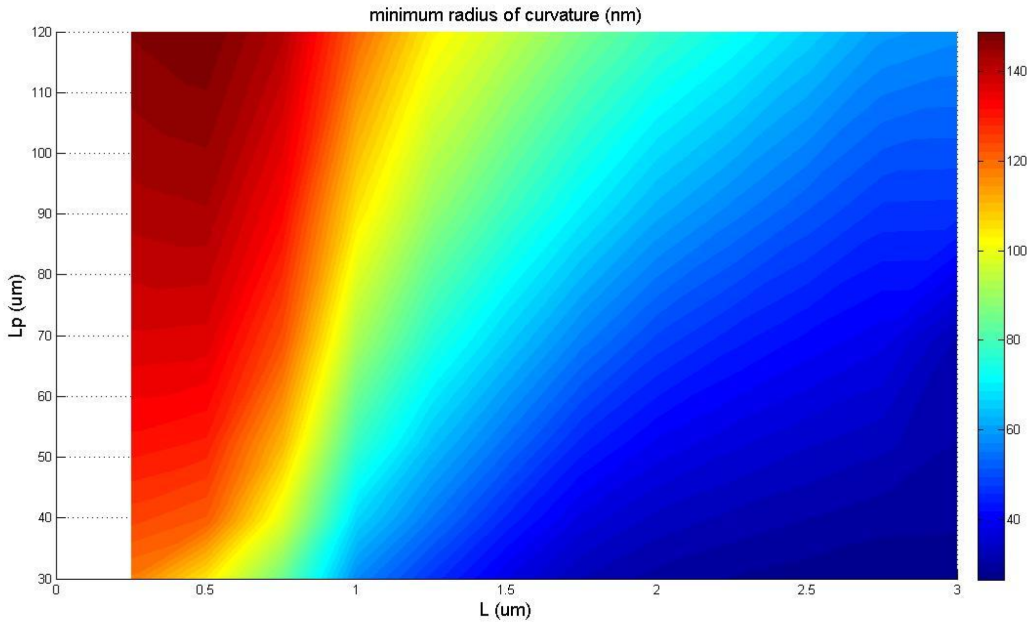

Fig. S8:

For d_i = 70 µm and P_{A0} = 4500 kPa, we simulate 960 CNTs at each value of L and L_p. The phase diagram depicts the minimum radius of curvature experienced by CNTs during the bubble cycle (averaged over all trials).

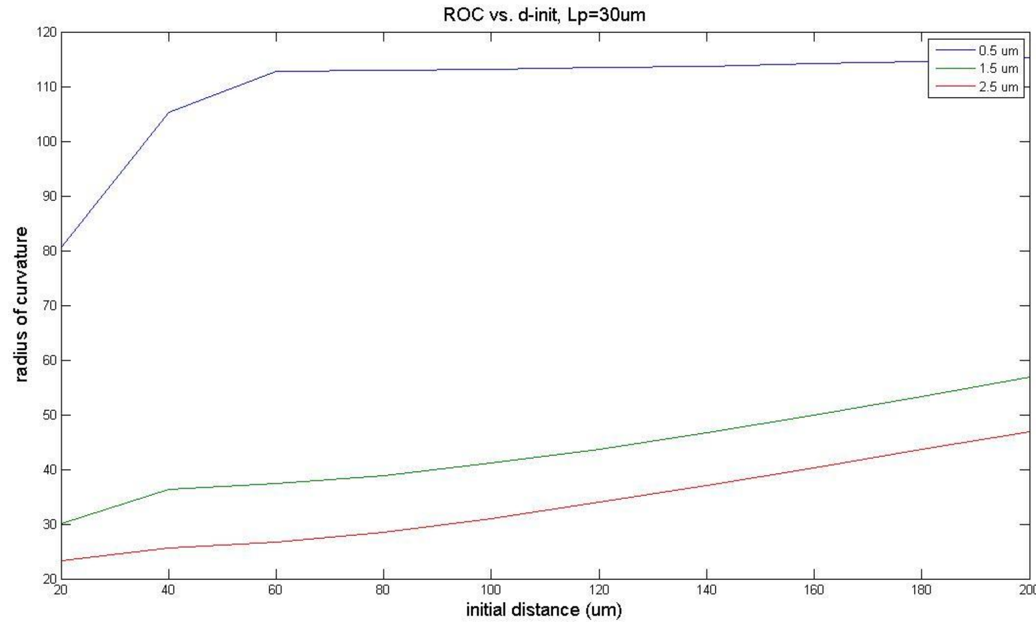

Fig S9:

For L_p = 30 μm and P_{A0} = 4500 kPa, we simulate 960 CNTs at each value of L and d_i. The diagram depicts the average of the minimum radius of curvature experienced by CNTs during the bubble cycle (averaged over all trials).

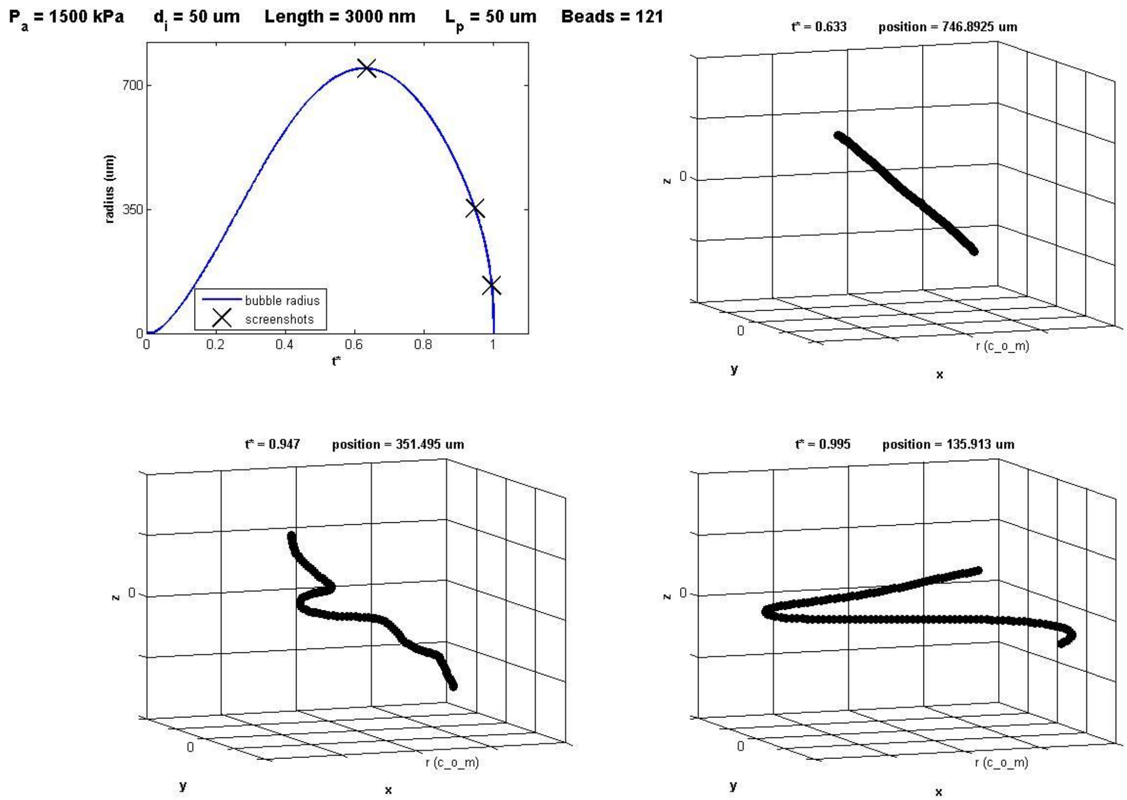

Fig S10:

Enlarged version of Fig. 4a.

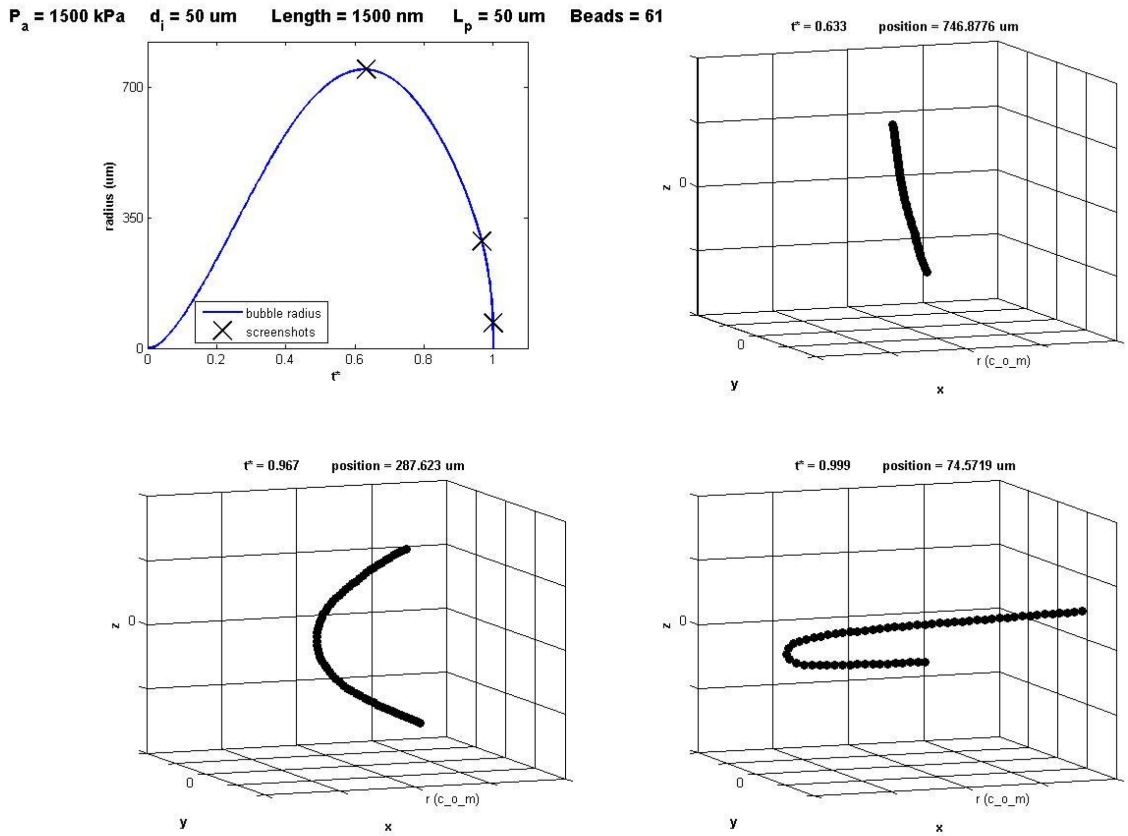

Fig S11:

Enlarged version Fig. 4b.

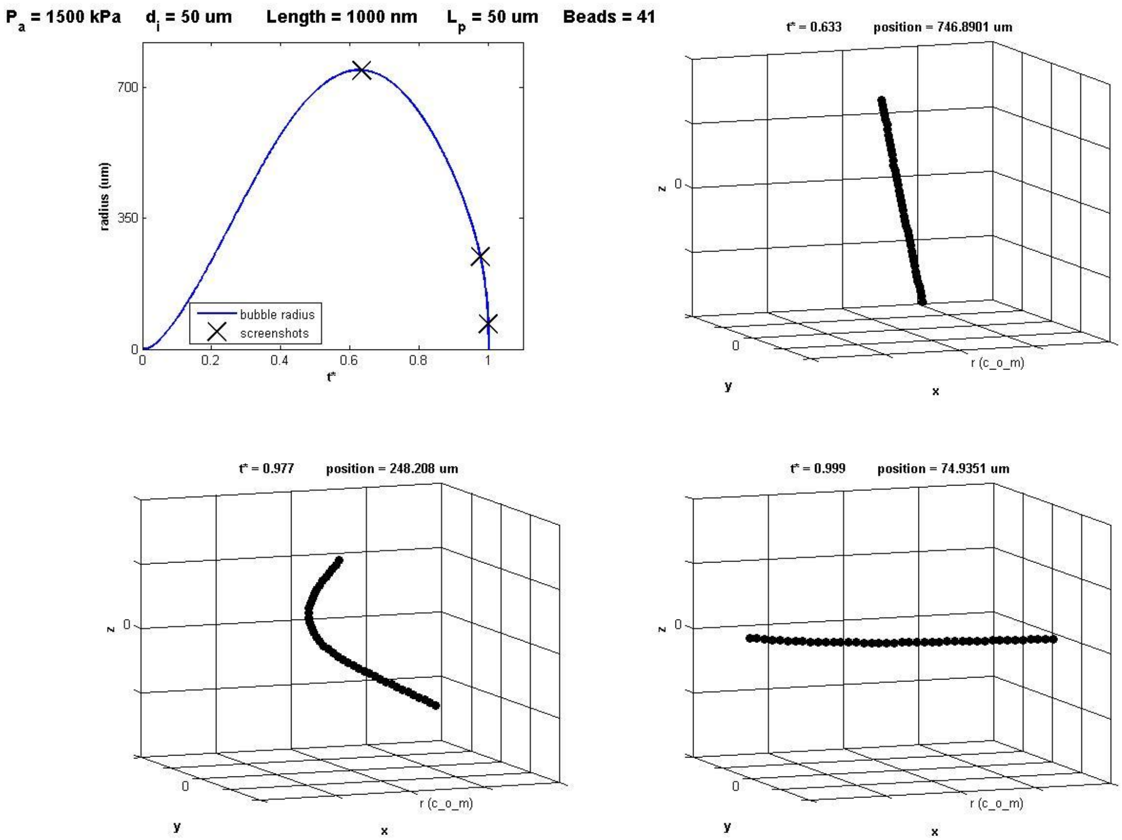

Fig S12:

Enlarged version of Fig. 4c.

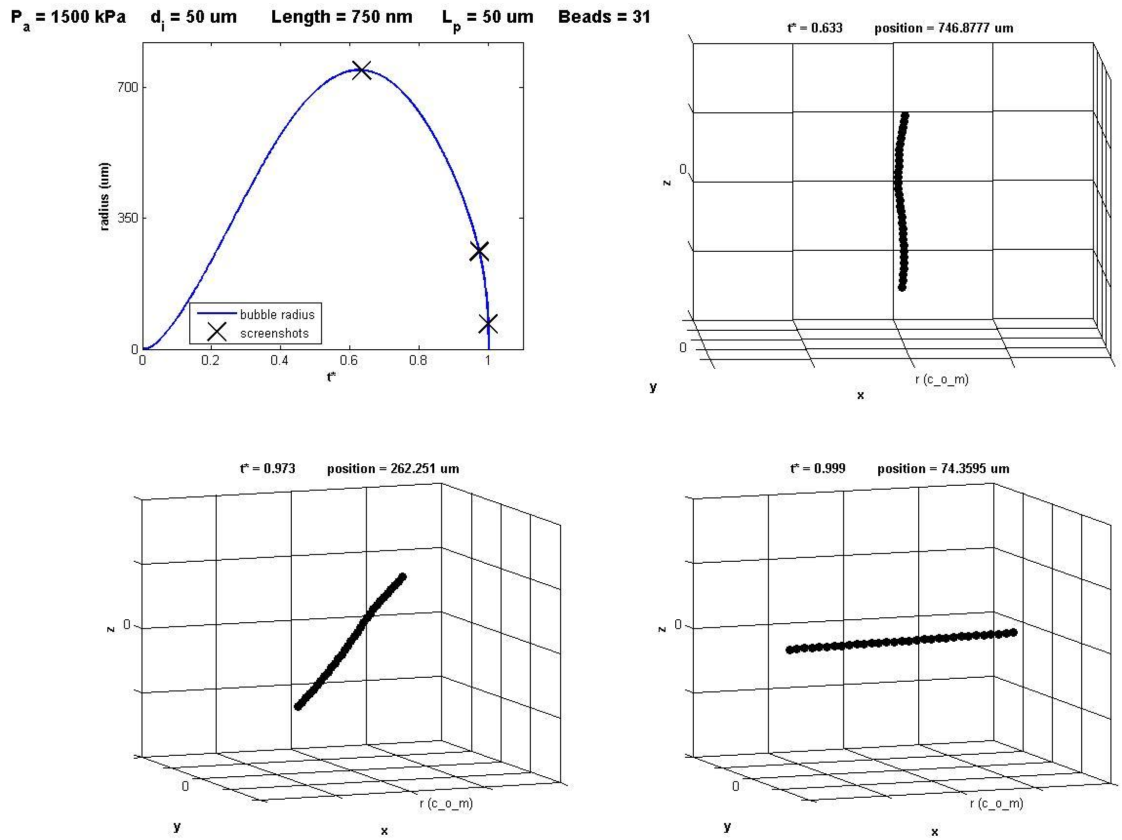

Fig S13:

Enlarged version of Fig. 4d.

REFERENCES

[1] A. Montesi, Interplay of Flow and Microstructure in Complex Fluids: Semiflexible Polymer Solutions and Emulsions, Chemical Engineering, Rice University, Houston, TX, 2005.
[2] G. Pagani, Modeling the dynamics of carbon nanotubes in sonicated fluids, M.S. Thesis, Facolta' di Ingegneria, Universita' di Bologna, Bologna, Italy, 2009.